An enhanced-sensitivity pure absorption gradient 4D ^{15}N, ^{13}C-edited NOESY experiment

D.R. Muhandiram, Guang Yi Xu and Lewis E. Kay

Protein Engineering Network Centres of Excellence and Departments of Medical Genetics, Biochemistry and Chemistry, University of Toronto, Toronto, Ontario, Canada M5S 1A8

SUMMARY

An enhanced-sensitivity gradient 4D ^{15}N,^{13}C-edited NOESY experiment is presented. Gradients are employed to suppress artifacts, eliminate the intense H_2O signal and select for the coherence transfer pathway involving ^{15}N magnetization. The latter use of the gradients results in a decrease in the number of phase cycle steps by a factor of two relative to the previously published 4D sequence (Kay et al., 1990) allowing for the recording of spectra with increased resolution per unit measuring time. Theoretical sensitivity enhancements of as much as a factor of $\sqrt{2}$ can be expected over the previously published sequence, neglecting the effects of relaxation and pulse imperfections.

Despite their relatively recent introduction into high-resolution NMR, pulsed field gradients have already found a number of important applications (Hurd and John, 1991; Vuister et al., 1992; John et al., 1993). The use of pulsed field gradients can result in spectra with excellent levels of water suppression, allowing, for example, the recording of H_2O spectra without the use of presaturation (Von Klienlin et al., 1991; John et al., 1992; Kay, 1993). This can result in significant improvements in spectral sensitivity, especially for peaks resonating at or near the water line or for resonances arising from labile protons. In addition, pulsed field gradients can be used to reduce the artifact content in spectra either by using gradients to select for particular coherence-transfer pathways (Maudsley et al., 1978; Bax et al., 1980; Hurd and John, 1991) or by eliminating undesired coherences at each step of a transfer path (Bax and Pochapsky, 1992). A reduction in the number of artifacts without a concomitant increase in the number of phase cycling steps is particularly important in 3D and 4D applications where, due to limitations in the total experimental acquisition time, there is often a trade-off between spectral resolution and the number of cycling steps possible. In this communication, all of the advantages of pulsed field gradients mentioned above are illustrated with an improved version of the 4D ^{15}N,^{13}C-edited NOESY experiment. Moreover, as is discussed below, sensitivity improvements relative to spectra recorded with the original 4D sequence (Kay et al., 1990) can be obtained.
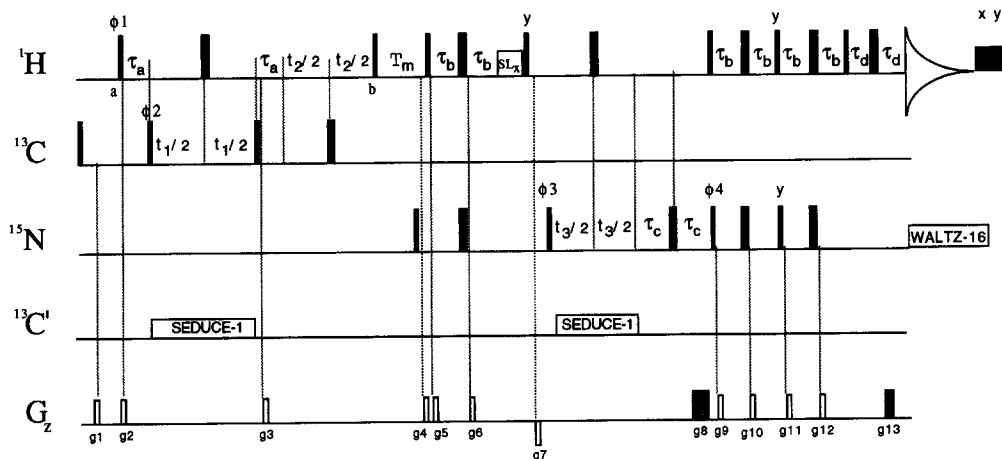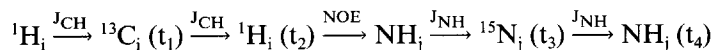
Fig. 1. Pulse sequence of the enhanced-gradient 4D ^{15}N,^{13}C-edited NOESY experiment. All narrow (wide) pulses have a flip angle of 90° (180°). The values of τ_a, τ_b, τ_c, τ_d and T_m were set to 3.3 ms, 2.4 ms, 1.5 ms, 0.5 ms and 150 ms respectively. Proton x,y purge pulses were applied after t_4 using an 8.5-kHz RF field for 8 ms (x) and 5 ms (y). These pulses aid in water suppression and ensure that magnetization has the same initial state at the start of each scan (Marion et al., 1989). The spin-lock pulse, SL_x was applied for 1 ms using an 8.5-kHz field (Messerle et al., 1989). The remaining ^{1}H pulses were applied using a 22-kHz field. All ^{13}C pulses were applied with an 18.5-kHz field with C' decoupling achieved using the SEDUCE-1 decoupling sequence at a field strength of 600 Hz (McCoy and Mueller, 1992a,b). ^{15}N pulses were applied using a 5.3-kHz field with ^{15}N decoupling during acquisition achieved with a 1-kHz WALTZ-16 decoupling sequence (Shaka et al., 1983). Quadrature detection in F_1 and F_2 was obtained via States-TPPI (Marion et al., 1989) of $\phi2$ and $\phi1$, respectively. The value of $\phi3$ and the phase of the receiver were incremented by 180° for each successive complex t_3 value. The phase cycle employed is: $\phi1$ = 45°; $\phi2$ = x,−x; $\phi3$ = x; $\phi4$ = x; Receiver = x,−x. For each t_3 value, N- and P-type coherences are obtained by recording datasets where the sign of g13 is inverted concomitantly with a 180° phase change in $\phi4$ (no change in the receiver phase). Note that only a single relative orientation of the gradients g8 and g13 will result in refocusing of magnetization for each $\phi4$ value. All of the gradients were applied along the z-axis. The durations and strengths of the gradients employed are: g1 = (1 ms,5 G/cm), g2 = g3 = (0.5 ms,8 G/cm), g4 = (3 ms,4 G/cm), g5 = g6 = (0.5 ms,8 G/cm), g7 = (1 ms,−10 G/cm), g8 = (1.25 ms,30 G/cm), g9 = g10 = (0.5 ms,8 G/cm), g11 = g12 = (0.5 ms,5 G/cm) and g13 = (0.125 ms, ± 27.8 G/cm). The value of g13 was optimized by maximizing the signal. The gradients are inserted in the sequence in such a way as to maximize the time between the application of a gradient pulse and the successive application of an RF pulse. We have found that on our system a minimum delay of 50 μs is necessary between a gradient and subsequent RF pulse in order to ensure that there is no sensitivity loss. The appropriate delays between gradients and pulses will vary between systems, however, and should be checked.

Figure 1 illustrates the enhanced-sensitivity gradient pulse scheme that has been used to record the 4D ^{15}N,^{13}C-edited NOESY experiment. The magnetization transfer pathway can be described concisely by:

$$^1H_i \xrightarrow{J_{CH}} {}^{13}C_i\ (t_1) \xrightarrow{J_{CH}} {}^1H_i\ (t_2) \xrightarrow{NOE} NH_j \xrightarrow{J_{NH}} {}^{15}N_j\ (t_3) \xrightarrow{J_{NH}} NH_j\ (t_4)$$

where the active couplings involved in each transfer step are indicated above the arrows. Gradients are used to suppress artifacts as well as to select for the coherence-transfer pathway involving ^{15}N magnetization during t_3. In the selection of ^{15}N magnetization using pulsed field gradients we have employed an enhanced-sensitivity approach (Kay et al., 1992; Muhandiram and Kay, 1993) based on enhanced non-gradient pulse schemes developed by Rance and co-workers (Cavanagh

et al., 1991; Palmer et al., 1991). A product operator description (Ernst et al., 1987) of the sequence of Fig. 1 shows that immediately prior to detection the magnetization of interest is given by:

$$M(t_1,t_2,t_3,z) = A \cos(\omega_C t_1) \cos(\omega_H t_2) \{H_y \cos(\theta_1) + H_x \sin(\theta_1)\}, \phi4 = x$$

$$M(t_1,t_2,t_3,z) = A \cos(\omega_C t_1) \cos(\omega_H t_2) \{-H_y \cos(\theta_1) + H_x \sin(\theta_1)\}, \phi4 = -x$$

(1)

where H_x and H_y are the x and y components of NH magnetization and A is a constant which is dependent on the efficiency of transfer of magnetization between the participating spins. The value θ_1 is given by $\theta_1 = \omega_N t_3 + \gamma_N B^1(z)\tau_1 \pm \gamma_H B^2(z)\tau_2$ for $\phi4 = \pm x$, where ω_N is the ^{15}N Larmor frequency, γ_i is the gyromagnetic ratio of spin i and τ_i (i = 1,2) is the duration of the z gradient pulse generating a magnetic field of magnitude B^i at position z in the sample. In the derivation of Eq. 1, $\phi1 = \phi2 = x$ and the effects of relaxation and pulse imperfections have been neglected. Assuming (i) that the gradients used to select for ^{15}N magnetization (g8 and g13) are sufficiently strong so that each of the gradients causes complete dephasing of magnetization; and (ii) that for $\phi4 = \pm x$ the gradients are adjusted so that $\gamma_N B^1(z)\tau_1 = \mp \gamma_H B^2(z)\tau_2$, Eq. 1 reduces to

$$M(t_1,t_2,t_3,z) = A \cos(\omega_C t_1) \cos(\omega_H t_2) \{H_y \cos(\omega_N t_3) + H_x \sin(\omega_N t_3)\}, \phi4 = x$$

$$M(t_1,t_2,t_3,z) = A \cos(\omega_C t_1) \cos(\omega_H t_2) \{-H_y \cos(\omega_N t_3) + H_x \sin(\omega_N t_3)\}, \phi4 = -x$$

(2)

For each value of t_3, datasets are recorded with $\phi4 = x$, $\gamma_N B^1(z)\tau_1 = -\gamma_H B^2(z)\tau_2$ and $\phi4 = -x$, $\gamma_N B^1(z)\tau_1 = \gamma_H B^2(z)\tau_2$ and stored in separate memory locations in a manner analogous to the recording of the x and y components of magnetization using the method of States (States et al., 1982). The data recorded with $\phi4 = x$ and $\phi4 = -x$ for a given value of t_3 are added and subtracted in a postacquisition manner to yield an amplitude-modulated dataset of the form:

$$M(t_1,t_2,t_3,z) = 2A \cos(\omega_C t_1) \cos(\omega_H t_2) \{H_x \sin(\omega_N t_3)\}, \text{(SUM)}$$

$$M(t_1,t_2,t_3,z) = 2A \cos(\omega_C t_1) \cos(\omega_H t_2) \{H_y \cos(\omega_N t_3)\}, \text{(DIFFERENCE)}$$

(3)

Because the SUM data is proportional to H_x at the start of the acquisition period while the DIFFERENCE data is proportional to H_y, a 90° zero-order phase correction is applied in the acquisition dimension to either the SUM or DIFFERENCE data prior to Fourier transformation.

A similar calculation to that given above shows that if the HSQC portion of the pulse scheme is not of the enhanced-sensitivity type (Cavanagh et al., 1991; Palmer et al., 1991) but gradients are still used to select for ^{15}N magnetization during t_3 in a manner suggested by Boyd et al. (1992), Davis et al. (1992) and Tolman et al. (1992), the signal intensity is reduced by a factor of two, relative to the present experiment. Alternatively, a calculation of the maximum sensitivity enhancement that can be obtained using the enhanced-sensitivity gradient 4D $^{15}N,^{13}C$-edited NOESY sequence relative to the original 4D $^{15}N,^{13}C$-edited NOESY sequence (Kay et al., 1990) which does not employ gradients to select for coherence-transfer pathways shows that signal-to-noise (S/N) enhancements of up to a factor of $\sqrt{2}$ can be obtained (Kay et al., 1992; Muhandiram

and Kay, 1993). This can be understood by recognizing that the process of adding and subtracting the N-type and P-type datasets to give SUM and DIFFERENCE data results in an increase in the signal by a factor of two over signal intensities observed in the unenhanced, nongradient experiment. However, the process of adding and subtracting the data will increase the noise floor by a factor of $\sqrt{2}$ (Palmer et al., 1991). Thus, the net increase in S/N is $\sqrt{2}$. A recent comparison of HNCO spectra acquired (a) using the sequence of Grzesiek and Bax (1992) with water suppression achieved via purge pulses and not presaturation; (b) using a sequence with ^{15}N coherence selection and water suppression achieved using gradients in the manner suggested by Davis et al. (1992), Boyd et al. (1992) and Tolman et al. (1992); and (c) using an enhanced-sensitivity sequence based on the Rance modification (Cavanagh et al., 1991; Palmer et al., 1991) with ^{15}N coherence-transfer selection and water suppression achieved with gradients shows average relative S/N ratios of 1.0(a):0.70(b):1.2(c) for four different proteins ranging in molecular weight from ~ 10 kDa to 20 kDa (Muhandiram and Kay, 1993). The extent of the enhancements is dependent on relaxation which occurs during the extra delays in the enhanced-sensitivity experiment and is also a function of the RF homogeneity profile of the probe since the enhanced sequence does involve an increased number of pulses.

The gradients g2–g7 and g9–g12 are applied in order to suppress potential artifacts arising from pulse imperfections. Application of the gradient pair (g2,g3) with $g2 = g3$ ensures that any transverse ^{1}H magnetization which is transferred to the z-axis by imperfections in the ^{1}H 180° pulse in the middle of the t_1 period is eliminated. In addition, transverse magnetization that does not experience the effects of this pulse is also removed by the action of the gradients. In a similar manner, the gradient pairs (g5,g6), (g9,g10) and (g11,g12) eliminate potential artifacts caused by pulse imperfections. The gradient g1 is applied immediately following the ^{13}C 90° pulse at the start of the pulse sequence. This eliminates magnetization originating from ^{13}C and ensures that the signal detected originates on ^{1}H. The gradient g4 is applied during the mixing period, T_m. Application of this gradient pulse ensures that any transverse magnetization present during T_m is effectively eliminated. This also includes transverse ^{15}N magnetization, generated by the application of the ^{15}N 90° pulse immediately prior to the gradient. The elimination of ^{15}N magnetization in this manner ensures that the ^{15}N signal present during t_3 originates exclusively from ^{1}H magnetization at the start of the experiment. Application of this gradient pulse towards the end of the mixing time allows radiation damping to bring the water signal completely back to the +z-axis (Smallcombe, S., personal communication). Immediately prior to the spin-lock pulse, SL_x, the desired magnetization is along the x-axis. Magnetization not parallel to the x-axis, including the water magnetization which is aligned along the y-axis, is scrambled by SL_x. The gradient pulse g7 is applied when the magnetization of interest is of the form H_zN_z, where H_z and N_z are the z-components of NH and ^{15}N magnetization respectively. Transverse magnetization is effectively eliminated at this point by g7. In addition, residual water in the transverse plane is also attenuated by the application of g7. Note that the gradients g7 and g8 are of opposite sign so that the effects of g7 and g8 are additive with respect to the elimination of water in the transverse plane (Bax and Pochapsky, 1992). As described previously, the use of g8 and g13 selects for the coherence-transfer pathway involving ^{15}N magnetization. It is therefore not necessary to cycle $\phi3$, which reduces the phase cycling in this experiment by a factor of two relative to the original 4D experiment (Kay et al., 1990).

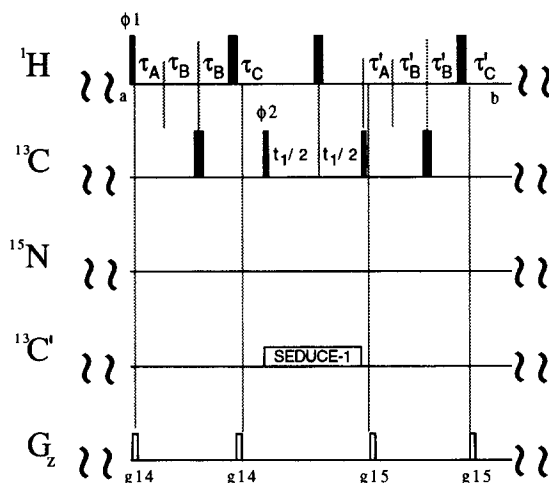In many triple-resonance experiments, ^{1}H magnetization is recorded in an indirect detection

Fig. 2. Pulse scheme of the 'shared time' gradient 4D $^{15}N, ^{13}C$-edited NOESY experiment. Only the portion of the sequence which differs from the sequence of Fig. 1 is shown. The region of the pulse sequence in Fig. 1 which extends from point a to point b is to be replaced with the partial sequence indicated in Fig. 2. The duration τ_{CH} is set to 1.65 ms. The gradients g14 and g15 are set to (100 µs,10 G/cm) and (100 µs,8 G/cm) respectively. As the lengths of g14 and g15 increase, the saving in the amount of time that ^1H magnetization spends in the transverse plane relative to the sequence of Fig. 1 decreases. It is therefore important to make the values of g14 and g15 short.

dimension prior to the transfer of the magnetization to a directly coupled heterospin, X. Recently Grzesiek and Bax (1993) and Logan et al. (1993) have described elegant improvements to these experiments whereby it is possible to combine the ^1H evolution period with the $^1H/X$ scalar transfer time and in this manner decrease the time during which ^1H magnetization is in the transverse plane by $1/(2J_{HX})$. In the case of the gradient 4D $^{15}N, ^{13}C$-edited NOESY it is possible to employ a similar strategy, resulting in a decrease in the total residence time of ^1H transverse magnetization of $\sim 1/J_{HX}$, albeit at the expense of one additional ^{13}C 180° pulse and two extra ^1H 180° pulses. Figure 2 illustrates the modified portion of the pulse scheme which combines the t_2 (^1H) evolution time with the $^1H/^{13}C$ scalar transfer time. The values τ_a, τ_b and τ_c are chosen according to

$$\tau_a = \tau_{CH} + n\zeta$$
$$\tau_b = n/(4\ SW2) - n\zeta$$
$$\tau_c = \tau_{CH} + 2\ pwc - n\zeta \qquad (4)$$
$$\zeta = (\tau_{CH} + 2\ pwc - g14)/(N-1)$$

where τ_{CH} is chosen to be slightly less than $1/(4J_{HC})$ to minimize losses from relaxation, pwc is the ^{13}C 90° pulse width, SW2 and N are the spectral width and the number of complex acquisition points in the ^1H dimension respectively, g14 is the duration of the pulsed field gradient applied during τ_c and n = 0,1,2...(N − 1) (i.e., n = 0 for the first complex t_2 point, 1 for the second and so forth). The increase in τ_a and decrease in τ_c results in the migration of the ^1H and ^{13}C 180° pulses applied before and after the t_1 period in Fig. 2 as a function of increasing t_2 while maintaining a constant $^1H/^{13}C$ scalar coupling evolution time. The values of τ_a', τ_b' and τ_c' can be obtained from Eq. 4 by replacing g14 with g15.
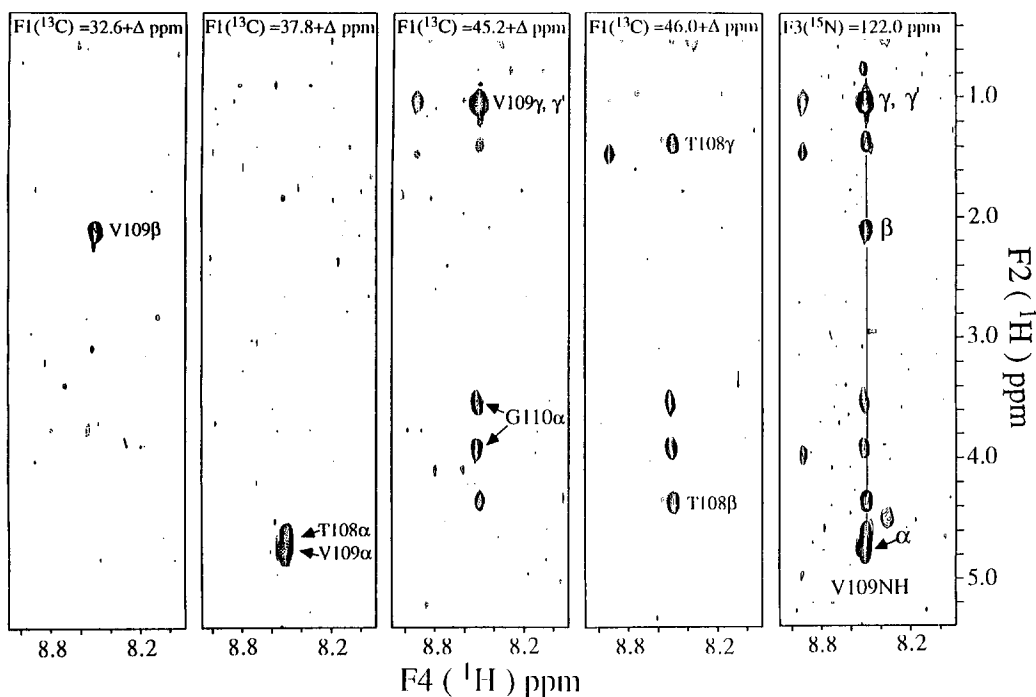
Fig. 3. Slices from the 4D dataset of CBD, 1.5 mM, pH = 7.0, T = 30 °C, at a ^{15}N chemical shift of 122.0 ppm showing the separation of NOE cross peaks to V109 NH. Note that because of the nearly identical ^{15}N and NH chemical shifts of V109 and G110, the G110α peaks also appear in some of the slices. The slice on the far right-hand side of the figure was obtained from a 3D dataset generated by taking the projection of the 4D spectrum onto the F_1 = 0 plane. A spectral width of 23.9 ppm was recorded in the ^{13}C dimension. Thus Δ = n · (23.9) ppm where n = 0, ± 1, ± 2 etc. Peaks in the carbon dimension which are folded an even number of times (n is even) are positive, while peaks folded an odd number of times are negative. For example, in the case of T108γ, Δ = −23.9 ppm, while for T108β, Δ = 23.9 ppm. In both cases, the cross peaks are folded once in the carbon dimension and hence are negative in the 4D spectrum. Negative cross peaks are indicated with dashed lines.

The gradient-enhanced 4D ^{15}N,[13]C-edited NOESY experiment was recorded on a Varian UNI-TY 500 MHz spectrometer equipped with a triple-resonance probehead with an actively shielded z-gradient and a gradient amplifier unit. The spectrum was acquired using a 1.5-mM sample of a fragment of a cellulase from *Cellulomonas fimi* (CBD, dimer consisting of monomers of 110 amino acids) in 90% H_2O/10% D_2O, pH = 7.0, T = 30 °C. The ^{1}H carrier was positioned at 3.8 ppm for the initial part of the sequence and subsequently switched during the mixing time to 8.7 ppm. The ^{13}C and ^{15}N carriers were positioned at 43 ppm and 119 ppm respectively for the duration of the experiment. Spectral widths in each dimension were 23.9 ppm (F_1), 8.0 ppm (F_2), 32.6 ppm (F_3) and 8.0 ppm (F_4). The data was acquired as a 16 × 64 × 16 × 256 complex matrix with a repetition delay of 0.9 s, a mixing time of 0.15 s and with two transients per FID, giving rise to a net recording time of ∼ 90 h. No presaturation was employed.

Figure 3 illustrates the quality of the data obtained. The data was processed using a combination of in-house written software and commercial software (NMRi, Syracuse, New York). In order to improve the resolution in the ^{15}N dimension, mirror-image linear prediction was employed (Zhu and Bax, 1990). The final absorptive part of the dataset consisted of a

$32 \times 128 \times 32 \times 512$ matrix. In the figure the slice at the far right-hand side was obtained from a 3D dataset generated by taking the projection of each ^{15}N cube of the 4D dataset onto the $F_1 = 0$ plane (corresponding to a ^{15}N-edited 3D NOESY spectrum). The remaining slices are extracted from the 4D dataset recorded with the sequence of Fig. 1. Each of the slices from the 4D dataset is at the same ^{15}N chemical shift as the slice from the 3D dataset. Note that because extensive folding was employed in the ^{13}C dimension along with a first-order phase correction of 180°, some of the cross peaks are negative. Although we have not recorded a 4D dataset using the modification indicated in Fig. 2, a preliminary comparison of 3D ^{15}N-filtered datasets recorded using the sequences of Figs. 1 and 2 with $t_1 = 0$, suggests that sensitivity improvements can be realized with the sequence of Fig. 2. The extent of the sensitivity gain for a particular protein is a function of the ^{1}H linewidths as well as the RF homogeneity of the probe.

In summary, in this communication we have presented a gradient-enhanced 4D ^{15}N,^{13}C-edited NOESY pulse sequence. The gradients are used to suppress water, to eliminate artifacts and for coherence-transfer selection. The use of gradients in this way enables a reduction in the number of phase-cycling steps by a factor of two (from four to two) relative to the original 4D ^{15}N,^{13}C-edited NOESY, thereby increasing the resolution that can be obtained for a given measuring time. This has important consequences in 4D spectroscopy where resolution in the indirectly detected dimensions is often limiting. The ability to suppress H_2O without resorting to presaturation schemes is particularly important for CBD, where for protein samples prepared at pH 7, presaturation results in a decrease in the entire spectral envelope by $\sim 40\%$. In addition, by using the sensitivity-enhancement approach described previously, enhancements of up to a factor of $\sqrt{2}$ beyond gains obtained by not using presaturation can be obtained relative to the previously published version of this sequence.

ACKNOWLEDGEMENTS

REFERENCES

Bax, A., De Jong, P.G., Mehlkopf, A.F. and Smidt, J. (1980) *Chem. Phys. Lett.*, **69**, 567–570.

Bax, A. and Pochapsky, S. (1992) *J. Magn. Reson.*, **99**, 638–643.

Boyd, J., Soffe, N., John, B.K., Plant, D. and Hurd, R. (1992) *J. Magn. Reson.*, **98**, 660–664.

Cavanagh, J., Palmer, A.G., Wright, P.E. and Rance, M. (1991) *J. Magn. Reson.*, **91**, 429–436.

Davis, A.L., Keeler, J., Laue, E.D. and Moskau, D. (1992) *J. Magn. Reson.*, **98**, 207–216.

Ernst, R.R., Bodenhausen, G. and Wokaun, A. (1987) *Principles of Nuclear Magnetic Resonance in One and Two Dimensions*, Clarendon Press, Oxford, pp. 25–32.

Grzesiek, S. and Bax, A. (1992) *J. Magn. Reson.*, **96**, 432–440.

Grzesiek, S. and Bax, A. (1993) *J. Biomol. NMR*, **3**, 185–204.

Hurd, R.E. and John, B.K. (1991) *J. Magn. Reson.*, **92**, 658–688.

John, B.K., Plant, D., Webb, P. and Hurd, R.E. (1992) *J. Magn. Reson.*, **98**, 200–206.

John, B.K., Plant, D. and Hurd, R.E. (1993) *J. Magn. Reson. Series A*, **101**, 113–117.

Kay, L.E., Clore, G.M., Bax, A. and Gronenborn, A.M. (1990) *Science*, **249**, 411–414.

Kay, L.E., Keifer, P. and Saarinen, T. (1992) *J. Am. Chem. Soc.*, **114**, 10663–10665.

470

Kay, L.E. (1993) *J. Am. Chem. Soc.*, **115**, 2055–2057.

Logan, T.M., Olejniczak, E.T., Xu, R.X. and Fesik, S.W. (1993) *J. Biomol. NMR*, **3**, 225–231.

Marion, D., Ikura, M., Tschudin, R. and Bax, A. (1989) *J. Magn. Reson.*, **85**, 393–399.

Maudsley, A.A., Wokaun, A. and Ernst, R.R. (1978) *Chem. Phys. Lett.*, **55**, 9–15.

McCoy, M. and Mueller, L. (1992a) *J. Am. Chem. Soc.*, **114**, 2108–2110.

McCoy, M. and Mueller, L. (1992b) *J. Magn. Reson.*, **98**, 674–679.

Messerle, B.A., Wider, G., Otting, G., Weber, C. and Wüthrich, K. (1989) *J. Magn. Reson.*, **85**, 608–613.

Muhandiram, D.R. and Kay, L.E. (1993) *J. Magn. Reson.*, in press.

Palmer, A.G., Cavanagh, J., Wright, P.E. and Rance, M. (1991) *J. Magn. Reson.*, **93**, 151–170.

Shaka, A.J., Keeler, J., Frenkiel, T. and Freeman, R. (1983) *J. Magn. Reson.*, **52**, 335–338.

States, D.I., Haberkorn, R.A. and Ruben, D.J. (1982) *J. Magn. Reson.*, **48**, 286–292.

Tolman, J.R., Chung, J. and Prestegard, J.H. (1992) *J. Magn. Reson.*, **98**, 462–467.

Von Kienlin, M., Moonen, C.T.W., Van der Toorn, A. and Van Zijl, P.C.M. (1991) *J. Magn. Reson.*, **93**, 423–429.

Vuister, G.W., Boelens, R., Kaptein, R., Burgering, M. and Van Zijl, P.C.M. (1992) *J. Biomol. NMR*, **2**, 301–305.

Zhu, G. and Bax, A. (1990) *J. Magn. Reson.*, **90**, 405–410.